ELSEVIER

Chemical Geology 177 (2001) 201–211

CHEMICAL GEOLOGY
INCLUDING ISOTOPE GEOSCIENCE

www.elsevier.com/locate/chemgeo

Estimating volcanic CO_2 emission rates from atmospheric measurements on the slope of Mauna Loa

Steven Ryan *

Mauna Loa Observatory, Climate Monitoring and Diagnostics Lab, NOAA, P.O. Box 275, Hilo, HI 96721, USA

Received 26 July 1999; accepted 9 March 2000

Abstract

The annual quiescent CO_2 emissions from the summit of Mauna Loa volcano between 1959 and 1999 were calculated from atmospheric measurements made 6 km downslope at the Mauna Loa Observatory (MLO). Volcanic CO_2 is trapped beneath a tens of meters thick temperature inversion at night and produces excess CO_2 mixing ratios of up to tens of ppm above background. Measurements of the excess CO_2, as a function of height above the ground, and wind direction are combined with the downslope wind speed to estimate the total flux of CO_2 trapped near the ground, which provides a minimum estimate of the total volcanic emissions. The CO_2 emissions were greatest shortly after each eruption and then decreased exponentially with $1/e$ time constants of 6.6, 6.5, and 1.6 years for the post-1950, 1975, and 1984 periods. Total emissions for these periods were 3.3, 1.9, and 2.5×10^8 kg, respectively. The distribution of quiescent volcanic CO_2 with wind direction shifted eastward after the 1975 and 1984 eruptions by a few degrees, coinciding with a shift in eruptive activity from the SW rift (1950) to the NE rift (1984). A broadening of the distribution in 1993–1995 and 1998 is interpreted as indicating a new source high on the SW rift. Published by Elsevier Science B.V.

Keywords: Carbon dioxide; Volcanic emissions; Flux; Mauna Loa

1. Introduction

Gas emission rates from erupting volcanoes are usually estimated by integrating the flux through a surface perpendicular to the axis of the plume. Ideally, this requires measurements of the gas mixing ratio and perpendicular wind velocity at every point where the plume passes through this surface, as well as measurements of the atmospheric background mixing ratio of the gas upwind of the volcano. In practice, a few measurements taken at intervals in space and time are averaged to approximate the flux. These measurements are usually taken either by remote sensors on the ground (e.g., COSPEC) or by in-situ sensors aboard aircraft. This paper describes the use of long-term in-situ measurements from a surface station to calculate time-averaged emission rates when the volcanic CO_2 is trapped beneath a surface temperature inversion.

CO_2 flux measurements in volcanic plumes are usually made from the air. Aircraft can carry high-precision analyzers to measure SO_2, CO_2, and other constituents in-situ (see papers in this volume). The instruments are usually flown in a series of successively higher traverses along a plane perpendicular to the plume axis (Gerlach et al., 1997). Winds are determined by the aircraft's instruments and more

* Fax: +1-808-933-6965.
E-mail address: ryan@mloha.mlo.hawaii.gov (S. Ryan).

0009-2541/01/$ - see front matter. Published by Elsevier Science B.V.
PII: S0009-2541(00)00392-2

recently, GPS. Plume mixing ratios of CO_2 range up to tens of ppm above an atmospheric background of around 360 ppm. The technique gives good results for eruptive plumes with large emission rates. Excess CO_2 in the plume can currently be measured to less than 1 ppm, corresponding to a minimum detectable emission rate of about 100–200 t/day (Gerlach, personal communication).

In this paper, volcanic CO_2 fluxes are calculated from yearly averaged measurements made on the ground at Mauna Loa Observatory (MLO) in Hawaii. Atmospheric CO_2 data from MLO provided the first proof that the CO_2 concentration of the global atmosphere was increasing (Pales and Keeling, 1965). The observatory is at an elevation of 3400 m, 6 km north of the 4169-m summit of Mauna Loa volcano. This is an excellent location to measure clean, background air minimally disturbed by distant anthropogenic and continental sources and sinks. After traveling across the Pacific for days to weeks, the well-mixed air parcels have a steady CO_2 mixing ratio with minute-scale variability typically less than 0.05 ppm (Ryan, 1995). The site is also a good location from which to monitor the quiescent emissions of Mauna Loa volcano. From the beginning of the MLO program, volcanic CO_2 coming from the summit was frequently detected in the atmospheric record (Pales and Keeling, 1965; Miller and Chin, 1978). Volcanic CO_2 only appears at night during periods of light winds. Under these conditions, radiative cooling produces a strong temperature inversion near the ground which traps the gas in a layer tens of meters thick (Ryan, 1997) and transports it to the observatory in downslope winds. The volcanic CO_2 is poorly mixed with background air upon reaching the observatory and is easily identified by a highly variable CO_2 trace and mixing ratio increases of up to tens of ppm. These events have always been regarded by atmospheric scientists as an undesirable contamination of the clean background signal and have been objectively eliminated from the climatological record (Keeling et al., 1976; Thoning et al., 1989). Ryan (1995) developed a methodology for estimating the volcanic emission rate from meteorological and atmospheric CO_2 measurements. The data were used to produce a continuous 37-year record of quiescent CO_2 outgassing, which spanned periods between the last three Mauna Loa eruptions in 1950, 1975, and 1984. Using other observatory measurements, a 20-year record of volcanic aerosols was derived, and upper limits on the amounts of volcanic H_2O, O_3, CH_4, SO_2, CO, and H_2 potentially present at MLO were determined.

In this paper, the relationship between local meteorology and the presence of volcanic CO_2 at MLO will be examined in more detail. The Mauna Loa CO_2 emissions record is refined and extended to the end of 1999 (42 years). New measurements of SO_2 and wind at several heights above the ground are used to better constrain the vertical distribution of volcanic gas. The relationship between volcanic CO_2 mixing ratio and wind direction is used to show that the location of the CO_2 source(s) near the summit has shifted after each eruption. These measurements also suggest that a weak new source appeared high on the SW rift in 1993–1995 and again in 1998.

2. Site and measurements

2.1. Site description

The Mauna Loa summit caldera is 3×5 km in diameter with a floor elevation of 4000 m at a bearing of 190° and distance of 6 km from MLO (Fig. 1). The northeast rift lies between 100° and

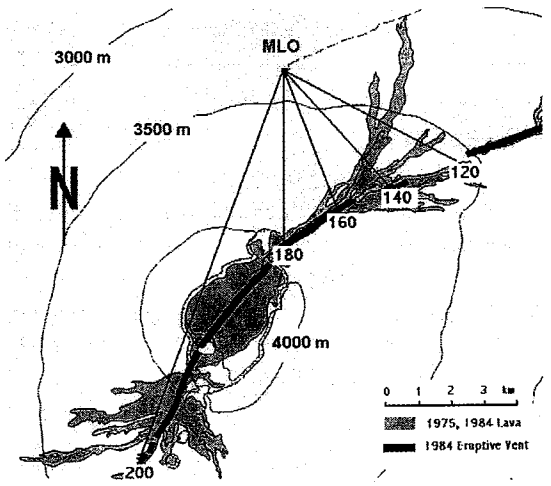

Fig. 1. Map of Mauna Loa summit area. North is up. The observatory (MLO) is located at 155.579°W 19.953°N. Radial lines from MLO give bearings in degrees from true north. Based on a figure from Lockwood et al. (1987).

180° at a minimum distance of 4 km, and the southwest rift is between 200° and 210° at distances greater than 10 km. Above an elevation of 2500 m, the slopes of Mauna Loa are barren of vegetation.

Between the 1975 and 1984 eruptions, visible fuming occurred along seven 120–362°C active fumaroles located on the 1975 eruptive fissure (Casadevall and Hazlett, 1983). Visible fuming ceased from this area after the 1984 eruption (Lockwood et al., 1987) and a much weaker source of visible fume was observed in the southwestern end of the caldera (J. Sutton, personal communication, 1993).

The height of the caldera rim varies from 180 m on the west side to near zero where it intersects the rifts to the NNE and SSW and forms two pits. During periods of light winds, the surface temperature inversion at night would tend to trap the emissions from the caldera basin and air would drain out of the caldera from the low points to the NNE or SSW depending on the prevailing wind direction. The observatory is located directly downslope from the NNE point.

2.2. CO_2 measurements

In 1958, the Scripps Institute of Oceanography (SIO) began monitoring CO_2 (Pales and Keeling 1965; Keeling et al., 1976) using an Applied Physics Corporation dual detector non-dispersive infrared analyzer. Air was sampled alternatively from intake lines at two different heights for 10 min each followed by a 10-min flow of reference gas. Water vapor was removed from the air stream by a −60°C freezer trap. The analyzer output voltage was recorded on a chart record, from which the data were hand scaled. The precision of the SIO system in measuring reference gases was between 0.1 and 0.2 ppm (Keeling, 1986).

In May 1974, what is now the National Oceanic and Atmospheric Administration (NOAA) Climate Monitoring and Diagnostics Laboratory (CMDL) began operating a Hartmann and Braun URAS-2 non-dispersive infrared analyzer. Every hour, two separate intake lines and two reference gases were sampled. The two reference gases were calibrated weekly by comparison with a suite of five standard gases. Water vapor was removed by a −60°C cold trap. Beginning in 1976, 1-min averages of the analyzer voltage output were recorded by a computer data acquisition and control system (Herbert et al., 1986). The precision of this system in measuring reference gases was between 0.015 and 0.03 ppm. In 1987, a Siemens Ultramat-3 analyzer was installed, which improved this precision to 0.009 ppm (Ryan, 1995).

The SIO and NOAA programs sampled air from various towers at heights ranging from 7 m (beginning in 1958) to 40 m (beginning in 1988). Air was always measured through at least two switched inlets every hour. There were periods when the inlets were at separate heights and other periods when they were at the same height (listed by Ryan, 1995).

2.3. SO_2 measurements

SO_2 was measured using a Thermo-Environmental Model 43-S pulsed-fluorescence analyzer from June 1994 to January 1997, and again from July 1998 to the present. The analyzer has a 95% response time of 2 min. The detection limit for a 20-min air measurement at the 95% confidence level is 50 ppt. The current system samples air through a thermostatically controlled heated Teflon line with inlet solenoids at 40, 23, 10, and 4 m above the ground. Every hour, these inlets are sampled for 6–7 min each in two consecutive sequences, followed by 10 min through a zero SO_2 filter. Hourly average mixing ratios are calculated for each of the four sampling levels. A single point calibration is made for 1 h each day.

3. Results

3.1. Volcanic emissions events at MLO

Two recent representative emissions events are shown in Fig. 2. On both nights, there were periods of steady background CO_2 mixing ratio with minute-scale variability of less than 0.05 ppm. When the emissions were present, the CO_2 mixing ratio increased by up to several ppm, and the minute-scale variability also increased greatly. At the same time, the SO_2 mixing ratio at the CO_2 sampling height (40 m) increased by 50–200 ppt above background levels of less than 50 ppt.

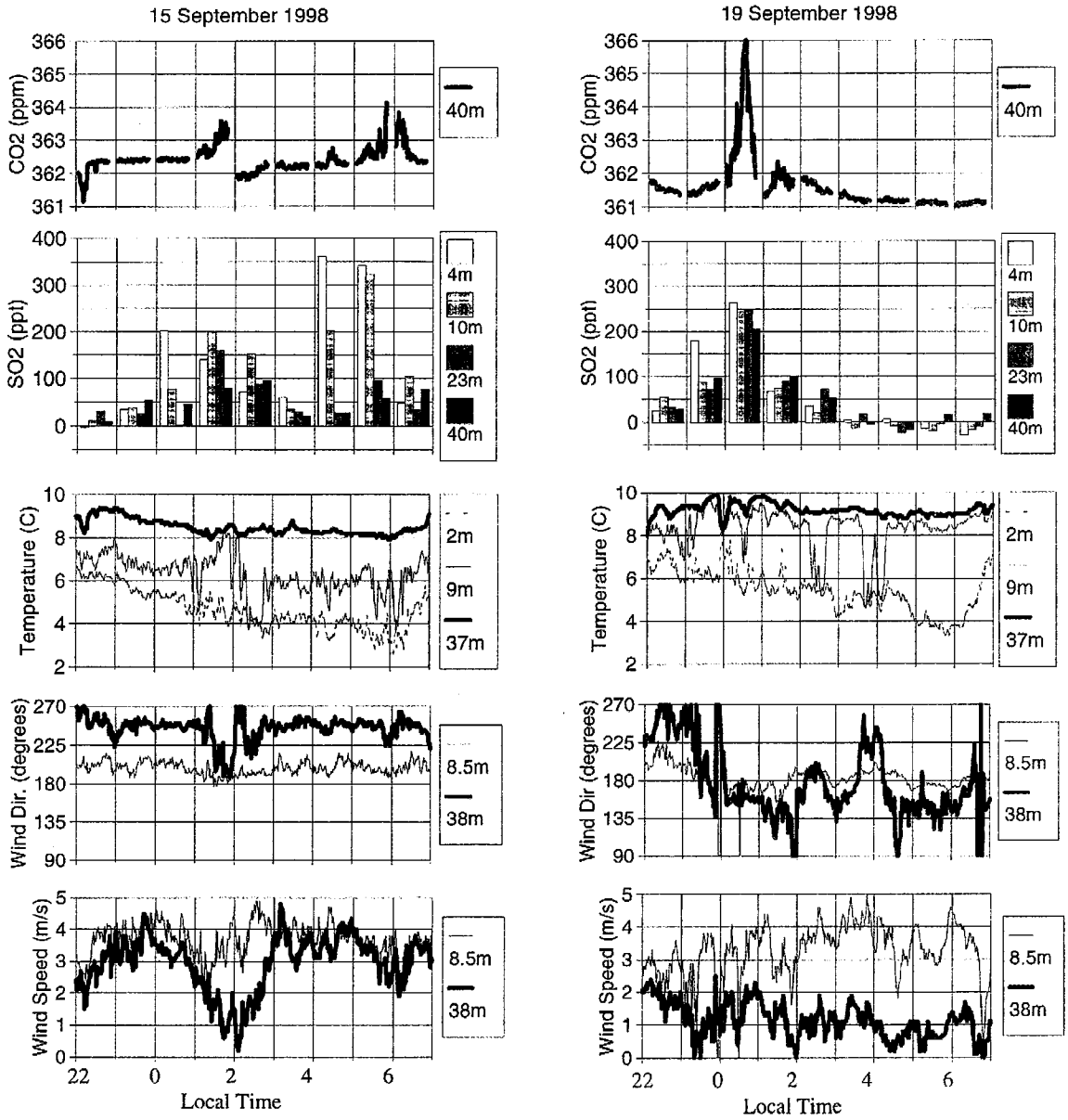

Fig. 2. Parameters measured at MLO on 2 nights at the indicated heights above the ground.

Ryan (1995) described a procedure for calculating the amount of excess volcanic CO_2 (termed ΔCO_2) from the continuous atmospheric measurements, which will be briefly reviewed here. The presence of emissions is identified by the amount of minute-scale variability in the CO_2 mixing ratio. This is measured by a parameter called the variability index (VI), which is the average absolute difference between all successive 1-min CO_2 mixing ratios during a sampling interval. For the NOAA data (Hofmann et al., 1998), there are two 22-min sampling intervals each hour. If the VI exceeds 0.1 ppm, emissions are

assumed to be present. Below 0.1 ppm is considered background. The background is estimated during an interval when emissions are present by linear interpolation between the nearest background mixing ratios that occurred during periods before and after. The interpolated background mixing ratio is then subtracted from the measured mixing ratio to obtain ΔCO_2.

By applying this methodology to the CO_2 data in Fig. 2, emissions were present during the hours of 1:00 AM, 5:00 AM, and 6:00 AM on September 15 with ΔCO_2 of 0.66, 0.38, and 0.43 ppm, respectively. On September 19, emissions were present during the hours of midnight and 1:00 AM with ΔCO_2 of 1.85 and 0.18 ppm.

The surface winds at MLO were described by Ryan (1997). The nighttime surface wind is composed of two components. These are a radiation wind, which is the downslope gravitational flow of radiatively cooled air near the ground, and a barrier wind that results when the winds in the free-troposphere flow around the mountain obstacle. These effects can be seen in the wind and temperature data in Fig. 2. On both nights, there was a strong temperature inversion near the ground, with the temperature difference between 2 and 37 m increasing from 3°C at 10 PM to 5°C at 6:00 AM. This produced a steady downslope radiation wind near the ground. At 8.5 m, the wind consistently blew downslope from 180 ± 20° at 3–4 m s^{-1} on both nights. Higher above the ground near the top of the temperature inversion, the wind is more dominated by the barrier wind field. The free-tropospheric wind direction at the 3400-m altitude of MLO can be estimated from radiosondes launched by the National Weather Service at 1:00 AM from nearby Hilo, HI. On September 15, the radiosonde wind reported at 3560 m (the measurement nearest 3400 m) was light, blowing from 274° at 1 m s^{-1}. This caused a westward deflection of the 38-m wind at MLO, which blew from about 250° at 3 m s^{-1}. On September 19, the radiosonde wind at 3301 m was blowing from 183° at 1.5 m s^{-1} while the 38-m wind at MLO was light (1 m s^{-1}) and variable, averaging 170°. On both nights, the free-tropospheric wind speed was low, which is a necessary condition for volcanic emissions from the summit to reach MLO because a strong easterly or westerly free-tropospheric wind blows the gas away from the direction of MLO and also tends to break up the surface temperature inversion (Ryan, 1997).

The thickness of the volcanic gas layer above MLO can vary substantially throughout the night as seen in the vertical distribution of volcanic SO_2 and the presence or absence of volcanic CO_2 at 40 m. The layer was less than 23 m thick during the hours of midnight, 4:00 AM, and 5:00 AM on September 15 (indicated by high SO_2 mixing ratios at 4 and 10 m, much lower mixing ratios at 23 and 40 m, and little or no volcanic CO_2 at 40 m). In contrast, the layer was more than 40 m thick during the hours of 1:00 AM on September 15 and midnight on September 19 (similar SO_2 mixing ratios at all levels, volcanic CO_2 present at 40 m).

3.2. Long-term record of volcanic CO_2 mixing ratio

Monthly average ΔCO_2 (described in Section 3.1) normalized to a common sampling height of 23 m is shown in Fig. 3. The averages are taken over all hours between midnight and 8:00 AM, and include hours when the emissions were absent (ΔCO_2 = zero). There were 117 h in the 4 years following the 1984 eruption when volcanic emissions caused some of the 1-min average CO_2 mixing ratios to exceed the upper range of the analyzer (usually about 25 ppm above ambient). These hours had a correction factor applied as described in Ryan (1995).

The fraction of hours that volcanic CO_2 was detected ranged from 50% shortly after the 1984 eruption to 15% in the late 1990s. Much of the

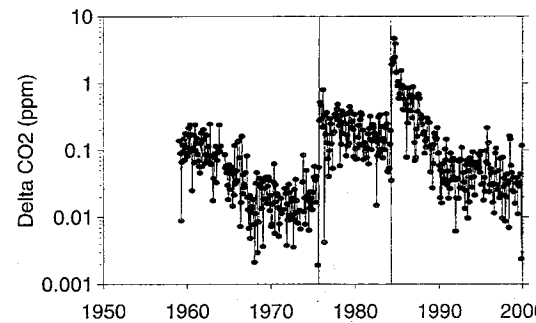

Fig. 3. Monthly average volcanic CO_2 23 m above Mauna Loa Observatory (ΔCO_2) from 1958 to 1999 between the hours of midnight and 7:00 AM. Hours with no volcanic CO_2 ($\Delta CO_2 = 0$) are included in the monthly averages.

scatter in Fig. 3 is caused by an annual cycle in the efficiency of transport of volcanic emissions to the observatory. Monthly average ΔCO_2 is least during the winter and spring seasons when strong free-tropospheric winds tend to deflect the emissions to the west of the observatory.

Fig. 3 shows that the volcanic CO_2 mixing ratio measured at MLO increased greatly after an eruption and then decreased exponentially in later years. Several other features were described by Ryan (1995) in the 1958–1995 records, which are briefly listed here. (1) There was a delay of 65 days between the end of the 1975 summit eruption and the onset of increased degassing. (2) No increase in ΔCO_2 was observed on short time scales (hours to weeks) prior to either eruption. (3) There was no increase in ΔCO_2 on a time scale of months-to-years prior to the 1984 eruption, but there was such an increase prior to the 1975 eruption. The magnitude of this increase was not great enough above the monthly noise level to provide an unambiguous eruption precursor.

3.3. Relationship between volcanic CO_2 and wind direction

Before 1977, wind speed and direction were recorded on charts and hand-scaled to produce hourly average values. The wind direction was only reported as N, NE, E, SE, etc. These measurements are combined with modern computer-recorded 1° resolution data after 1977 to show the annual average ΔCO_2 in three 45° wide sectors centered on wind directions of 135° (SE), 180° (S), and 225° (SW) for the complete 42-year record (Fig. 4A). The distribution has shifted after each eruption. Between 1958 and 1974, there was about three times as much volcanic CO_2 coming from the SW sector as from the SE sector. After the 1984 eruption, this ratio was closer to 1.

The direction of the center of the three-sector distributions is shown in Fig. 4B. The center direction has shifted eastward by 3.3° between the post-1950 and post-1984 quiescent periods (95% confidence error on the mean is $\pm 1.5°$). Although we do not understand the wind field at the summit well enough to pinpoint the source location(s) from these data, it appears that the average location of the

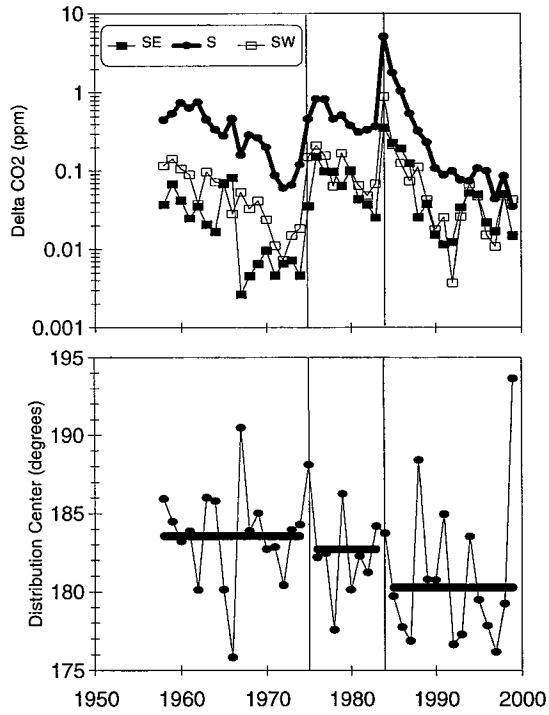

Fig. 4. A (top) — Yearly average volcanic CO_2 (ΔCO_2) partitioned by wind sector. Each sector is 45° wide, centered on the indicated direction. B (bottom) — Yearly average direction of the center of the distributions shown above.

quiescent CO_2 source region has shifted slightly from west to east following the last two eruptions. This is consistent with a shift in eruptive activity from the southwest rift (1950) to the summit (1975) to the northeast rift (1984).

An interesting feature in Fig. 4A is a flattening of the distribution that occurred between 1993 and 1995. In every year prior to 1993, the volcanic CO_2 mixing ratio in the SW and SE sectors was always 6–10 times less than that in the S sector. In 1994, the mixing ratio was nearly equal in all three sectors. This is seen more clearly in Fig. 5, which shows the ΔCO_2 distribution in 10° sectors. During the post-1975 quiescent period (1977–1983), the full-width at half-maximum of the distribution (FWHM) was 51° ($\sigma = 5°$). In the early post-1984 quiescent period (1984–1987), the FWHM was similar at 48° ($\sigma = 2°$). In contrast, the FWHM during the anomalous 1993–1995 period was 70° ($\sigma = 9°$). Ryan (1995) suggested that this was caused by additional emissions

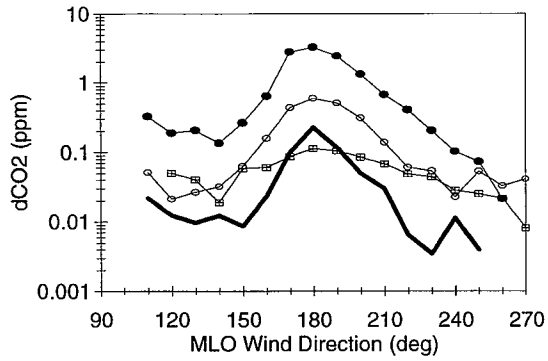

Fig. 5. ΔCO_2 distributions for 1984–1987 (filled circles), 1977–1983 (empty circles), 1993–1995 (squares), and 1990–1992 (no symbols, heavy line) as a function of the 8.5-m wind direction measured at MLO.

from a new source located near the opposite side of the summit caldera from MLO, possibly high on the SW rift. Gas coming from this location would have to travel equal distances around the mountain to arrive at MLO from either the southwest or southeast depending on the prevailing wind direction. If this interpretation is correct, this source was active in 1993–1995, diminished in 1996–1997, and became active again in 1998 (Fig. 4).

The prevailing wind direction in the free troposphere at the 4000-m altitude of the summit can be estimated from the daily 1:00 AM radiosonde wind measurements taken from nearby Hilo, HI. The free-tropospheric wind presumably directs the gas as it emerges from the vents near the summit. The relationship between this wind direction and nightly average ΔCO_2 is shown in Fig. 6. These data have more scatter than the MLO ΔCO_2 distribution in Fig. 5 because the wind direction determined from a drifting balloon has a much greater error than that from a surface wind vane, because the balloon wind at 4000 m is interpolated from various reported levels, and because the barrier wind field around the mountain is three-dimensionally complex. The volcanic CO_2 is greatest at MLO when the free-tropospheric wind blows from a southerly direction as expected, but it is only three to five times less when the free-tropospheric wind blows from the north. The FWHM of these distributions is about 120°. In 1977–1983, the distribution center was from 179°. After the 1984 eruption, the center shifted to the east to 166° in 1984–1989. This is consistent with the shift in eruptive activity from the summit (1975) to the northeast rift (1984). The anomalous period of 1993–1995 had a distribution center from 183° with relatively more volcanic CO_2 coming from southwestern free-tropospheric winds, which supports the hypothesis that there was a new source located high on the SW rift.

3.4. Average vertical gradient of the volcanic CO_2 layer

Since summit emissions are trapped beneath the surface temperature inversion at night, the mixing ratio of volcanic gas measured at MLO decreases with height above the ground. Although the thickness of this layer can vary substantially from hour to hour (Section 3.1), the vertical gradient averaged over many months or years is well defined (Fig. 7).

Ryan (1995) derived the vertical profile of the volcanic CO_2 layer at four heights (13, 16, 23, and 40 m). For 17 out of 37 years, CO_2 had been sampled from pairs of sampling lines at different heights. These data were used to calculate the ratio of ΔCO_2 at the four heights, normalized to a standard height of 23 m, shown as filled circles in Fig. 7.

In 1992–1993, wind and temperature were measured at six heights on the sampling tower (2.5, 5, 10, 20, 30, and 38 m). During this 2-year period, a subset of 23 nights was selected when radiosonde

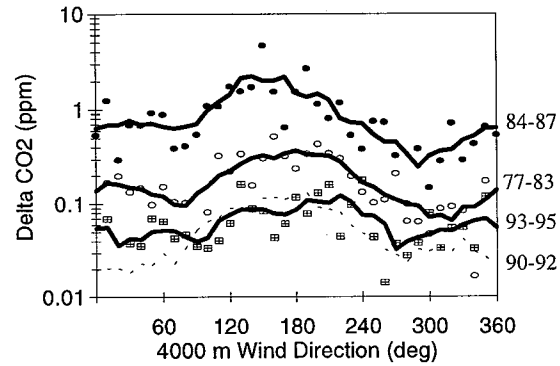

Fig. 6. ΔCO_2 distributions for 1984–1987 (filled circles), 1977–1983 (empty circles), 1993–1995 (squares), and 1990–1992 (no symbols, dashed line) as a function of the wind direction measured by Hilo radiosondes in the free-troposphere at 4000 m altitude. The lines are five-point running means.

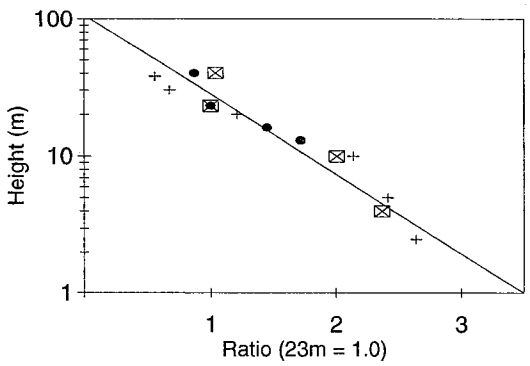

Fig. 7. The average vertical profile of volcanic CO_2 (filled circles), volcanic SO_2 (rectangles), and wind speed (crosses). Each is ratioed to the average value at 23 m above the ground. Details of the derivations are given in the text.

measurements showed that the free-tropospheric wind was light (<1 m s^{-1}) at 3400 m, which is a favorable condition for transport of volcanic CO_2 to MLO. The average downslope component of the wind at each level was calculated between midnight and 7:00 AM (Ryan, 1997). These wind speeds, normalized to the interpolated wind speed at 23 m, are shown as crosses in Fig. 7.

The 1998–1999 SO_2 program made measurements at four sampling heights (4, 10, 23, and 40 m). During the first 300 days of operation, there were 21 nights in which the CO_2 data showed that Mauna Loa emissions were present between midnight and 7:59 AM, and an SO_2 baseline of less than 50 ppt indicated that pollution from Kilauea was absent. An average background SO_2 mixing ratio of 40 ppt was obtained for these nights by averaging the SO_2 mixing ratio at 40 m for all hours in which $\Delta CO_2 = 0$. The volcanic SO_2 mixing ratios at the four sampling heights were calculated by taking the average mixing ratio at each height and subtracting the 40 ppt background. These values, normalized to the mixing ratio at 23 m, are plotted as rectangles in Fig. 7.

The final result shows that the vertical gradient is consistent between all three measurements. Volcanic CO_2, volcanic SO_2, and downslope wind speed are all proportional and decrease inversely with the logarithm of height above the ground between 2.5 and 40 m. The regression fit through all the data in Fig. 7 has $r^2 = 0.91$. The integrated area under the curve is equal to a 78-m column having a uniform ratio of 1.0. This confirms the result (79 m) that was reported in 1995 using only the CO_2 data.

3.5. Average wind speed

The two-component (downslope and cross-slope) wind at 8.5 m above the ground was selected for all hours between midnight and 7:00 AM in which volcanic CO_2 was present (ΔCO_2 was greater than zero). These were combined into annual averages between 1977 and 1998. The overall average downslope component for this period was 3.7 m s^{-1} ($\sigma =$ 0.4) m s^{-1}. The average cross-slope (westerly) component was only 0.2 ($\sigma = 0.2$) m s^{-1}. Ninety percent of the time that volcanic CO_2 was present, the wind speed was less than 6.5 m s^{-1}.

3.6. Estimated volcanic CO_2 flux

The observatory measurements are used to make annual estimates of the total CO_2 flux that is trapped beneath the temperature inversion at night. By averaging the data over a period of 1 year, variability arising from changing meteorological conditions on time scales from minutes to seasons is minimized. It is assumed that the volcanic CO_2 is contained within a wedge-shaped segment with its origin at the summit, and a radius of 6 km (equal to the summit–MLO distance). The downslope vertical face of this segment is the normal surface through which the flux passes. The total flux through this face was calculated on a computer spreadsheet by numerical integration, using the results of the previous sections.

The flux calculation goes as follows. At the 680 mbar pressure and 10°C temperature of MLO, 1 ppm of CO_2 is equivalent to 1.06×10^{-6} kg m^{-3}. The mixing ratio of volcanic CO_2 and the wind speed as a function of height above the ground are both given by the linear fit in Fig. 7. Using ΔCO_2 at a reference height of 23 m and the average downslope wind speed of 3.7 m s^{-1} at a height of 8.5 m, the vertical integral for the flux is 1.98×10^{-4} kg m^{-1} s^{-1} ppm^{-1}. The total flux is obtained by integrating horizontally using annual average ΔCO_2 distributions such as those in Fig. 5. Unfortunately, accurate wind direction data was only available after 1977. Before this, winds were recorded in 45° sectors. To

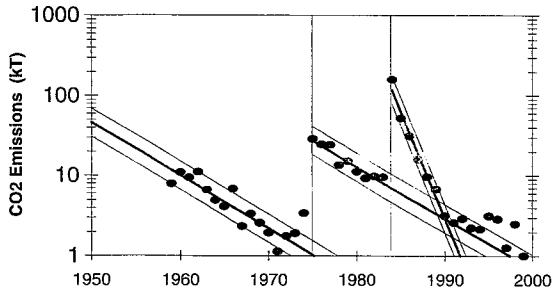

Fig. 8. Estimated minimum annual CO_2 emissions from the Mauna Loa summit. The heavy lines give logarithmic regression fits to the 1960–1973, 1975–1983, and 1984–1989 periods. The parameters of these regressions are in Table 1. The light lines contain 95% of the annual averages from 1959 to 1990 (Section 4.1). 1 kT = 10^6 kg.

produce consistent results, the annual average ΔCO_2 in the 45° sector centered on 180° must be used for the horizontal integration throughout the 42-year period of record. Fortunately, this is a reasonable approximation, since the average FWHM of the distributions between 1977 and 1997 was found to be 50° (Section 3.5). A 45° sector corresponds to an arc length of $2\pi \times 6000$ m $\times (45°/360°)$, which is equal to 4710 m. The total flux is therefore 0.93 kg s^{-1} ppm^{-1}. Over 1 year, a 1-ppm average volcanic CO_2 mixing ratio from the south sector equals a total emission of 2.9×10^7 kg of CO_2. This is somewhat less than the 3.7×10^7 kg obtained earlier by Ryan (1995) using simpler assumptions.

Annual CO_2 emissions for each calendar year are given in Fig. 8. The values for 1975 and 1984 are averages for the 12 months following the end of the eruptions, which occurred in July and April, respectively. Logarithmic regressions were calculated for each of three post-eruptive periods. The parameters of the regressions are listed in Table 1, where the fit to the 1960–1973 data was extended back to 1950 to obtain estimates for the initial rate and total emissions for that period.

4. Discussion

4.1. Do the CO_2 fluxes represent total emissions?

The values in Fig. 8 represent the total emissions of CO_2 from the Mauna Loa summit only if the volcanic gas remains completely trapped beneath the temperature inversion at night (midnight to 7:00 AM). To the extent that some CO_2 may escape from beneath the inversion within 6 km of the summit, these estimates must be considered a lower limit of the total CO_2 emissions. For the gas to remain completely trapped, the heat flux at the vents/fumaroles must not be great enough to loft any of the CO_2 above the surface temperature inversion near the point of emission. If this condition is not met, a gradual decrease in the quiescent heat flux from the vent following an eruption could introduce a systematic error in the CO_2 emissions estimates, with the greatest underestimation occurring shortly after the eruption. There is also the potential for some volcanic gas to leak from beneath the inversion layer in transit downslope to MLO. The MLO meteorological measurements show that the local inversion layer is fully formed by midnight on average (Ryan, 1997), when the volcanic CO_2 mixing ratio is proportional to the downslope wind speed (Fig. 7). Substantial variations in the vertical distribution of wind and temperature sometimes occur on time scales of minutes to hours (Fig. 2), and some volcanic CO_2 could be lost when the steady flow is disrupted.

The annual CO_2 emissions estimates are scattered about the exponential fits in Fig. 8. Between 1959 and 1990, half of the points are within a factor of

Table 1
Minimum total CO_2 emissions estimates

Period	r^2	$1/e$	Σ Emissions 10^8 kg	Year 1 emissions 10^8 kg	Lava volume 10^8 m^3
1960–1973	0.85	6.6	3.3 (est.)	0.46	3.76
1975–1983	0.89	6.5	1.9	0.27	0.30
1984–1989	0.97	1.6	2.5	1.18	2.20

13% (between $F \times 1.13$ and $F/1.13$) of the regression value F, and 95% of the points are within a factor of 49% of the regression. The 95% confidence band is plotted in Fig. 8. The scatter is most likely dominated by annual variations in average meteorological conditions but could also be caused by departures of the volcanic emission rate from a steady exponential decrease.

4.2. Interpreting emissions after 1994

After the 1984 eruption, the summit CO_2 emission rate rose to 160 kt year^{-1}, and then fell exponentially with $1/e = 1.6$ years. At this rate of decrease, emissions should have fallen below 1 kt year^{-1} after 1991 and become undetectable by the late 1990s (Fig. 8). Instead, the emissions after 1991 resumed the trend established after the 1975 eruption, which had a much slower decay rate. Based on the data through 1994, Ryan (1995) proposed that this was evidence for the presence of two independently degassing sources after 1984. In this model, the post-1975 source ($1/e = 6.5$ years) was not disturbed by the 1984 eruption. The 1984 eruption produced an independent source of CO_2 with a rapidly decaying emission rate ($1/e = 1.6$ years) which fell below that of the post-1975 source after 1990.

The five additional years of measurements reported here (1995–1999, Fig. 8) are consistent with this hypothesis. Two years (1997 and 1999) were within the 95% confidence band of the post-1975 fit and 3 years (1995, 1996, and 1998) were above it. In two of the years with higher emissions (1995 and 1998) there was also an increase in volcanic CO_2 from the SE and SW directions (Fig. 4), which was interpreted in Section 3.3 as coming from another, intermittent source located high on the SW rift.

In the model of Johnson (1995), the 4-km deep Mauna Loa reservoir is charged with CO_2-rich parental magma during an eruption, which then degasses as a batch with a characteristic exponentially-decaying rate. If the reservoir remains open to the atmosphere and stays at a fixed depth, this exponentially-decaying rate would define the minimum level of all future emissions. The annual summit emissions since 1990 have never fallen below the post-1975 trend (Fig. 8), which would be expected if they reflect the degassing of a batch of magma put in place by the 1975 eruption.

4.3. Background ΔCO_2 and the future

In the future, emissions from the current reservoir should continue to decay with $1/e = 6.5$ years. In the absence of a new eruption or the emergence of a significant new source of volcanic CO_2, the issue of what constitutes a background level of ΔCO_2 will become important in interpreting future data. Besides Mauna Loa volcano, there are other known and potential sources of variability in the atmospheric CO_2 mixing ratio (Ryan, 1995). Sources of noise such as synoptic shifts in the background mixing ratio and rare instrumental instability contribute both positive and negative changes in ΔCO_2 and have a long-term sum of zero. There is the potential for contamination from island sources of CO_2 such as respiration from vegetation at elevations below 2000 m and emissions from Kilauea volcano below 1200 m elevation. These sources have minimal impact on ΔCO_2 since they are distant and/or diffuse and their emissions become relatively well-mixed with background air by the time they reach the observatory. Under average nighttime conditions, these emissions remain trapped below the base of the trade wind inversion which has an average altitude of 2130 m (Ryan, 1997). At night, air from lower altitudes is more likely to reach the observatory when winds have large easterly or westerly components than when the winds are southerly (directly downslope). This would produce a background ΔCO_2 distribution having the opposite shape of those in Fig. 5, with a minima at 180°.

The upper limit of the annual average background level of ΔCO_2 is 0.005 ppm, which was observed in the SE sector between 1969 and 1974 (Fig. 4). This is certainly an over estimate of the background because the SE sector winds were carrying some emissions from Mauna Loa during this period. At the current $1/e$ decay rate of 6.5 years, the annual average south (summit) sector ΔCO_2 mixing ratio will fall to 0.005 ppm by the year 2014. Thus, in the absence of an eruption, we can expect to make useful measurements of the CO_2 emissions of Mauna Loa for at least another decade.

5. Conclusions

Atmospheric CO_2 measurements and wind measurements made between 1958 and 1999 at MLO can be used to calculate the annual average flux of volcanic CO_2 trapped beneath the surface temperature inversion at night. This flux provides a lower-limit estimate of the emissions from the summit of Mauna Loa volcano. The emission rates were greatest shortly after an eruption and then decayed exponentially, with $1/e$ time constants of 6.6, 6.5, and 1.9 years for the post-1950, 1975, and 1984 quiescent periods. Total CO_2 emissions calculated for these periods were 3.3, 1.9, and 2.5×10^8 kg, respectively.

A shift in eruptive activity from the SW rift (1950) to the summit (1975) to the NE rift (1984) was accompanied by a several degree eastward shift in the peak of the wind direction distribution of quiescent volcanic CO_2. In 1993–1995 and 1998, there was an unprecedented broadening of the distribution, which could be explained by the appearance of a new source of CO_2 high on the SW rift. These features are also seen in the distribution of volcanic CO_2 with wind direction in the free troposphere at 4000 m measured by nearby radiosondes.

The annual emissions data suggests that the post-1975 CO_2 source was not affected by the 1984 eruption, which apparently established a second, independently degassing source. The post-1984 source ($1/e = 1.6$ years) was exhausted faster than the post-1975 source ($1/e = 6.5$ years) and produced less CO_2 after 1990. Between 1991 and 1999, CO_2 emissions followed the trend observed after the 1975 eruption, with slight increases in 1995–1996 and 1998.

Acknowledgements

The MLO staff has diligently made measurements for over 40 years, particularly J.F.S. Chin who has operated the CO_2 program since the early 1960s. The Scripps Institute of Oceanography CO_2 measurements at MLO were begun by C.D. Keeling and sustained by D.J. Moss and others. The NOAA/CMDL CO_2 data were obtained through the efforts of P. Tans, K. Thoning, L.S. Waterman, and others. The NOAA/CMDL condensation nuclei measurements were begun by B. Bodhaine and are currently overseen by J. Ogren.

References

Casadevall, T.J., Hazlett, R.W., 1983. Thermal areas on Kilauea and Mauna Loa volcanoes, Hawaii. J. Volcanol. Geotherm. Res. 16, 173–188.

Gerlach, T.M., Delgado, H., McGee, K.A., Doukas, M.P., Venegas, J.J., Cardenas, L., 1997. Application of the LI-COR CO_2 analyzer to volcanic plumes: a case study, Volcan Popocatepetl, Mexico, June 7 and 10, 1995. J. Geophys. Res. 102, 8005–8019.

Herbert, G.A., Green, E.R., Harris, J.M., Koenig, G.L., Roughton, S.J., Thaut, K.W., 1986. Control and monitoring instrumentation for the continuous measurement of atmospheric CO_2 and meteorological variables. J. Atmos. Ocean Tech. 3, 414–421.

Hofmann, D.J., Peterson, J.T., Rosson, R.M. (Eds.) 1998. Climate Monitoring and Diagnostics Laboratory No. 24: Summary Report 1996–1997. NOAA Environmental Research Laboratories, Boulder, CO.

Johnson, D.J., 1995. Gravity changes on Mauna Loa Volcano. In: Rhodes, J.M., Lockwood, J.P. (Eds.), Mauna Loa Revealed: Structure, Composition, History, and Hazards. Geophys. Monogr. vol. 92. AGU, Washington, DC, pp. 127–143.

Keeling, C.D., 1986. Atmospheric CO_2 Concentrations — Mauna Loa Observatory, Hawaii 1958–1986. NDP-001/R1. Carbon Dioxide Information Center, Oak Ridge National Laboratory, Oak Ridge, TN.

Keeling, C.D., Bacastow, R.B., Bainbridge, A.E., Ekdahl Jr., C.A., Guenther, P.R., Waterman, L.S., Chin, J.F.S., 1976. Atmospheric carbon dioxide variations at Mauna Loa Observatory, Hawaii. Tellus 28 (6), 538–551.

Lockwood, J.P., Dvorak, J.J., English, T.T., Koyanagi, R.Y., Okamura, A.T., Summers, M.L., Tanigawa, W.R., 1987. Mauna Loa 1974–1984: a decade of intrusive and extrusive activity. In: Decker, R.W. (Ed.), Volcanism in Hawaii. U.S. Geol. Surv. Prof. Pap. vol. 1350, pp. 537–570, Chap. 19.

Miller, J.M., Chin, J.F.S. et al., 1978. Short-term disturbances in the carbon dioxide record at Mauna Loa Observatory. Geophys. Res. Lett. 5, 669–671.

Pales, J.C., Keeling, C.D., 1965. The concentration of atmospheric carbon dioxide in Hawaii. J. Geophys. Res. 70, 6053–6076.

Ryan, S.C., 1995. Quiescent outgassing of Mauna Loa volcano 1958–1994. In: Rhodes, J.M., Lockwood, J.P. (Eds.), Mauna Loa Revealed: Structure, Composition, History, and Hazards. Geophys. Monogr. vol. 92. AGU, Washington, DC, pp. 95–116.

Ryan, S.C., 1997. The wind field around Mauna Loa derived from surface and balloon observations. J. Geophys. Res. 102 (D9), 10711–10725.

Thoning, K.W., Tans, P.P., Komhyr, P.P., 1989. Atmospheric carbon dioxide at Mauna Loa Observatory: 2. Analysis of the NOAA GMCC Data, 1974–1985. J. Geophys. Res. 94 (D6), 8549–8565.